

Structural Shape Optimization Considering Both Performance and Manufacturing Cost

William Nadir* and Il Yong Kim†
Massachusetts Institute of Technology, Cambridge, MA

Olivier L. de Weck‡
Massachusetts Institute of Technology, Cambridge, MA

This paper presents a structural shape optimization method that considers not only structural performance but also manufacturing cost. Most structural optimizations only take into account structural performance metrics such as stress, mass, deformation, or natural frequency. However, it is often observed that structural performance improves at the expense of manufacturing cost. This work explores the tradeoff between mass and manufacturing cost with the application of the abrasive water jet (AWJ) manufacturing process. Structural performance, defined as maximum von Mises stress, is a constraint in this work. Work-in-progress results are presented for two structural design examples to demonstrate this tradeoff between mass and manufacturing cost while investigating shape optimization using non-uniform rational B-splines (NURBS). Additional work is still needed to complete this research project.

Nomenclature

C	= Abrasive waterjet (AWJ) cutting speed estimation constant
C_{man}	= Total manufacturing cost, [\$]
d_m	= Mixing tube diameter of the AWJ cutting machine, [in]
d_o	= AWJ cutter orifice diameter, [in]
E	= AWJ cutter error limit
f_a	= Abrasive factor for abrasive used in AWJ cutter
h	= Thickness of material machined by AWJ, [in]
J	= Objective function
L_j	= Step length for j^{th} step along cut curve
m	= Number of curves being optimized in the structure
M	= Part structural mass, [kg]
M_a	= AWJ abrasive flow rate, [lb/min]
n_i	= Number of control points for the i^{th} curve
$N_{i,k}$	= NURBS basis function of degree k for i^{th} knot
N_m	= Machinability number
OC	= Overhead cost for machine shop, [\$/hr]
P_i	= Knot coordinates for i^{th} NURBS control point
P_w	= AWJ water pressure, [ksi]
q	= AWJ cutting quality
R	= Arc section cut radius for AWJ cutter, [in]
S_i	= Total number of steps along i^{th} cutting curve
u_{as}	= AWJ arc section cutting speed approximation, [in/min]

* Graduate Research Assistant, bnadir@mit.edu, Department of Aeronautics and Astronautics, Room 33-409, 77 Massachusetts Ave., Cambridge, MA, AIAA Student Member.

† Postdoctoral Associate, Department of Aeronautics and Astronautics, Room 33-409, 77 Massachusetts Ave., Cambridge, MA.

‡ Assistant Professor, Department of Aeronautics and Astronautics and Engineering Systems Division, Room 33-410, 77 Massachusetts Ave., Cambridge, MA, AIAA Senior Member.

u_{max}	=	AWJ maximum linear cutting speed approximation, [in/min]
x	=	Vector of X-coordinate design variables
y	=	Vector of Y-coordinate design variables
α	=	Weighting factor used in objective function
δ	=	Deflection [mm]
σ	=	Stress [Pa]

I. Introduction

TYPICAL structural design optimization involves the optimization of important structural performance metrics such as stress, mass, deformation, or natural frequencies. This structural design method often does not consider an important factor in structural design: manufacturing cost. In this research, manufacturing cost is considered as an important performance metric, in addition to typical structural performance metrics. The multiobjective optimization technique, weighted sum method, is used to observe the tradeoff between manufacturing cost and structural performance. While it is not possible to make a manufacturing cost model that represents all manufacturing processes, the scope of this research has been limited to one manufacturing process: rapid prototyping by an abrasive water jet (AWJ) cutter. Although AWJ cutting is the manufacturing process considered in this paper, this multiobjective structural performance versus manufacturing cost framework is generalizable to other manufacturing processes.

A. Literature Survey

The aim of structural optimization is to determine the values of structural design variables in order to minimize an objective function of a structure while satisfying given constraints. Structural optimization may be subdivided into shape optimization and topology optimization. For shape optimization, the theory of shape design sensitivity analysis was established by Zolésio and Haug.^{1,2} Bendsøe and Kikuchi³ proposed the homogenization method for structural topology optimization by introducing microstructures and applied it to a variety of problems.⁴ Yang et al. proposed artificial material and used mathematical programming for topology optimization.⁵ Kim and Kwak first proposed design space optimization, in which the number of design variables and layout change during the course of optimization.⁶

Structural shape optimization has been performed along with an estimation of manufacturing cost by Chang and Tang.⁷ This work involved optimization of three-dimensional parts to reduce mass and manufacturing cost for the special application of the fabrication of a mold or die. However, manufacturing cost was not included in either the objective or constraint function, as is done in this paper. Park *et al.* performed optimization of composite structural design considering mechanical performance and manufacturing cost.⁸ This work focused on the optimal stacking sequence of composite layers as well as the optimal injection gate location to be used in the composite material manufacturing process. However, as in the work by Chang and Tang, Park et. al. did not perform multidisciplinary optimization including manufacturing cost.

The weighted sum method is a popular method for handling objective functions with more than one objective. Objective functions with many different linear combinations of the individual objectives are optimized in order to obtain a Pareto front. Zadeh⁹ performed early work on the weighted sum method. In addition, Koski¹⁰ used the weighted sum method for the application of multicriteria truss optimization.

The standard method for determining manufacturing cost for an AWJ cutter has been presented by Zeng and Kim¹¹ as well as Singh and Munoz.¹² To estimate manufacturing cost, Zeng and Kim used the cutting speed of the water jet cutter multiplied by an overhead cost factor for the specific AWJ cutting machine being used.

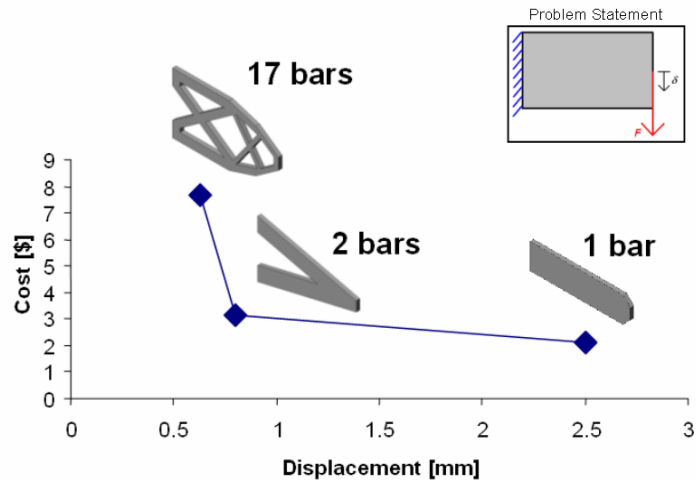


Figure 1: AWJ manufacturing cost versus structural performance.

AWJ cutting speed prediction models have been presented by Zeng and Kim.¹³ Zeng and Kim developed a widely accepted AWJ cutting speed prediction model. Zeng has also worked out the theory behind AWJ cutting process.¹⁴ Zeng, Kim, and Wallace¹⁵ conducted an experimental study to determine the machinability numbers of engineering materials to be used in water jet machining processes.

For the purposes of this paper, the AWJ cutting speed model presented by Zeng and Kim is used. The Zeng and Kim model has been used by Singh and Munoz to predict AWJ cutting speed and is also used, in part, in Omax water jet CAM software.^{16,17}

The goal of this research is to do structural shape optimization, considering manufacturing cost as an important performance metric. The manufacturing process of abrasive water jet is used as the manufacturing process for our research. The tradeoff between structural performance and manufacturing cost is explored in this paper. An example of this tradeoff is shown in Fig. 1.

Figure 1 shows a plot of AWJ manufacturing cost versus displacement for three parts with identical mass, material properties, and boundary and loading conditions. Displacement is used in this illustrative example as the structural performance metric. Manufacturing cost for this example is determined using the same cost model presented later in this paper.

It can be seen that as manufacturing cost increases with part complexity, so does the structural performance benefit resulting from this increased complexity. Depending on the importance placed on manufacturing cost and structural performance, an optimal design could be chosen from design options along a curve similar to the one shown in Fig. 1. If structural performance is considered to be significantly more important than manufacturing cost, a design would likely be chosen from the left-hand side of the curve. If, on the other hand, an inexpensive design without strict structural performance requirements is desired, a design near the right-hand portion of the curve would likely be selected. Finally, if a structural design with a balance between manufacturing cost and performance is desired, a design located near the knee of the curve, located near the two-bar example, would likely be chosen.

While other researchers have performed structural shape optimization and investigated manufacturing cost, a lack of research exists for true multidisciplinary optimization considering both structural performance and manufacturing cost. This paper presents multidisciplinary structural shape optimization considering both structural performance and manufacturing cost.

II. Problem Statement

The multiobjective optimization problem statement is shown below. The weighted sum method is used for the multiobjective problem.

$$\min J(x_j^i, y_j^i) = \alpha M + (1 - \alpha) C_{man} \quad (1)$$

subject to

$$\sigma_{\max} \leq \sigma_c \quad (2)$$

with

$$x_{j, LB}^i \leq x_j^i \leq x_{j, UB}^i \quad (3)$$

$$y_{j, LB}^i \leq y_j^i \leq y_{j, UB}^i \quad (4)$$

where

$$i = 1, \dots, m$$

$$j = 1, \dots, n_m$$

where J is the objective function, M is the structural mass, C_{man} is the total estimated manufacturing cost of the structure, x and y are the design vectors composed of the X and Y-coordinates of the j^{th} control point for the i^{th} NURBS curve, respectively, and α is the weighting factor for the two objectives. In addition, n_i is the total number

of control points for the i^{th} curve, and m is the total number of curves being optimized in the structure. Finally, σ_{max} is the maximum von Mises stress in the structure and $x_j^{i, LB}$, $x_j^{i, UB}$, $y_j^{i, LB}$, and $y_j^{i, UB}$ are the side constraints for the design vector variables. These side constraints are usually different for each design variable given the nature of the problems being optimized.

III. Theory

A. Optimization Method

The optimal structural design for the given design requirements is determined using an optimization approach shown in Fig. 2. The optimization algorithm used for this design optimization is a gradient-based optimization algorithm. This algorithm, used in the MATLAB¹⁸ function *fmincon*, a sequential quadratic programming-based optimizer, is used. The fact that the cost model is also a MATLAB module and MATLAB can communicate with the structural analysis software made the algorithm a suitable choice for this problem.

The initial design, defined using X and Y , is input to the system and the objective function is evaluated using finite-element analysis (FEA) and the manufacturing cost model developed for the application of abrasive waterjet cutting. Structural performance evaluation using finite-element analysis is performed using the ANSYS software package.¹⁹

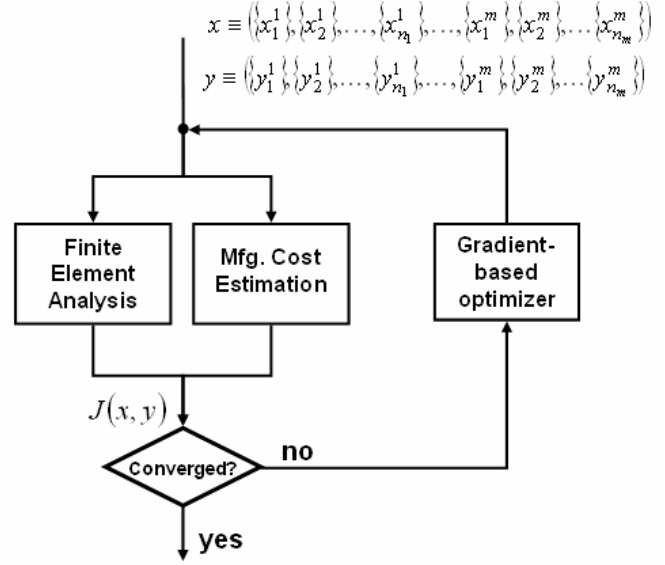


Figure 2: Shape optimization flow chart.

B. Manufacturing Cost Estimation

The manufacturing method used to estimate manufacturing cost is abrasive waterjet cutting. This manufacturing method uses a powerful jet of a mixture of water and abrasive and a sophisticated control system combined with Computer-Aided Machining (CAM) software. This allows for accurate movement of the cutting nozzle. The end result is a machined part with possible tolerances ranging from ± 0.001 to ± 0.005 inches. It is possible for AWJ cutting machines to cut a wide range of materials including metals and plastics.

The inputs to this AWJ manufacturing cost estimation module include the design vector variables and parameters such as material properties, and material thickness. The output of this module is the manufacturing cost to make the desired cuts using AWJ.

Based on the material thickness and material properties, a maximum cutting speed is determined for the AWJ cutter. An important assumption can be made that the cutting speed of the waterjet cutter is constant throughout most of the cutting operation when the radius of curvature is large enough. In reality, the cutting speed of waterjet will slow if any sharp corners or curves with small arc radii lie in the cutting path. The equation for the maximum linear cutting speed of the AWJ cutter is shown in Equation (5). The overhead cost associated with using the AWJ cutting machine, OC , is shown in Equation (6).

$$u_{\max} = \left(\frac{f_a N_m P_w^{1.594} d_o^{1.374} M_a^{0.343}}{C q h d_m^{0.618}} \right)^{1.15} \quad (5)$$

$$OC = \$75 / \text{hr} \quad (6)$$

where f_a is an abrasive factor, N_m is the machinability number of the material being machined, P_w is the water pressure, d_o is the orifice diameter, M_a is the abrasive flow rate, q is the user-specified cutting quality, h is the material thickness, d_m is the mixing tube diameter, and C is a system constant that varies depending on whether metric or Imperial units are used.

However, many of the curves in a typical manufacturing example are not linear. This issue requires a modification to the linear cutting speed estimation equation in order to estimate the cutting speed along cut curves with an arc section radius, u_{as} . The modification to Equation (5) involves using Equation (7) to replace the quality factor, q . This modification takes the radius of curvature of the cut curve, R , into account. The resulting cutting speed estimation equation is shown in Equation (8).

$$q = \frac{0.182h}{(R + E)^2 - R^2} \quad (7)$$

$$u_{as} = \left(\frac{f_a N_m P_w^{1.594} d_o^{1.374} M_a^{0.343} [(R + E)^2 - R^2]^{1.15}}{0.182Ch^2 d_m^{0.618}} \right) \quad (8)$$

where E is the error limit. In practice, the error limit is set by experience and judgment. However, for the purposes of this project, an error limit of 0.001 is used.²⁰

Total manufacturing cost is estimated using Equation (9).

$$C_{man} = OC \left[\sum_{i=1}^m \left(\sum_{j=1}^{S_i} \frac{L_j}{u} \right) \right] \quad (9)$$

where L_j is the length of the j^{th} step along the cutting curve, u is the AWJ cutting speed, either arc section or maximum linear cutting speed, and S_i is the total number of steps along the cutting curve for the i^{th} curve.

In order to validate the results of the manufacturing cost estimation model, results from the model are compared to Omax results for an identical manufacturing scenario. Omax contains an accurate manufacturing cost estimator and is a good benchmarking tool for this application. The short cantilevered beam, a commonly used structure to benchmark optimization methods, is used to validate the results of the manufacturing cost model. A screenshot of the Omax result is shown in Fig. 3. Figure 4 is the output of the MATLAB AWJ cost estimation model. The darker the color of the cutting path, the slower the waterjet cutting speed.

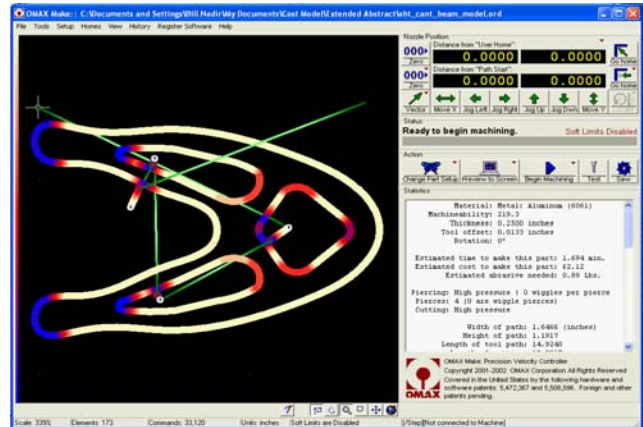


Figure 3: Omax output screenshot.

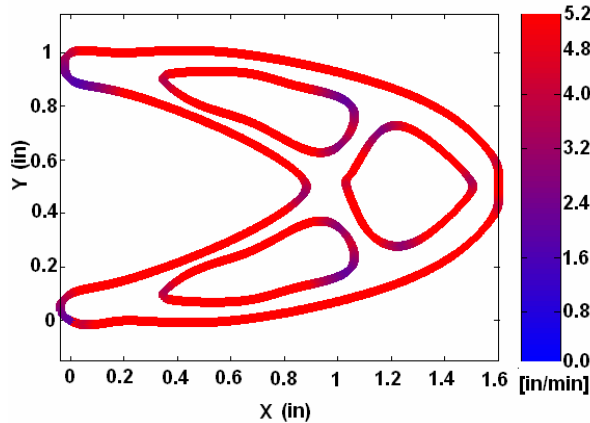


Figure 4: AWJ cost model output.

Table 1: Manufacturing cost estimation module results.

	Omax	Cost Model
Manufacturing Time (min)	1.69	1.71
Manufacturing Cost	\$2.14	\$2.11

The results of the software validation shown in Table 1 shows that the MATLAB manufacturing cost estimation software accurately estimates the manufacturing cost for abrasive waterjet cutting.

IV. Results

A. Generic Structural Part Design Optimization

1. Initial Design

Shape optimization considering both structural performance and manufacturing cost is performed for a generic metallic structural part shown in Fig. 5. The material selected for this example is A36 Steel with a Young's modulus of 200 GPa, a Poisson's ratio of 0.26, and a yield strength of 250 MPa. The evenly-distributed pressure across the top of the part is 3.7×10^7 N/m². The bottom line of the part is fixed in all translations and rotations. A factor of safety of 1.5 was assumed for this example. ANSYS elastic shell elements with a defined material thickness of 1 cm are used for the static analysis.

Three holes are cut in the metallic part and the shape of these holes is controlled by four control points each. It is assumed that the hole locations and rough side constraints are previously determined by topology optimization. Examples of this are shown in Fig. 7. The cutting path created by the control points is determined using NURBS curves created in ANSYS.

Non-uniform rational b-spline curves (NURBS) are used to describe the cut curves in the part. NURBS curves are chosen for their ability to control the shape of a curve on a local level by each of the defined control points, or knots. A complex shape can be represented with little data in the form of several of these control points. The NURBS formulation used is a proprietary ANSYS formulation. The generic NURBS formulation equation is below.

$$P(u) = \frac{\sum_{i=0}^n h_i P_i N_{i,k}(u)}{\sum_{i=0}^n h_i N_{i,k}(u)} \quad (10)$$

In Equation (10), $P_i(u)$ is the position vector of the i^{th} control point at time u and n is the total number of control points used to define the curve. The homogeneous coordinate of the i^{th} control point is h_i and $N_{i,k}$ is the basis function for the NURBS curve of degree k for the i^{th} control point.

The side constraints for each of the control points are shown in Fig. 6. The side constraints are restricted to these small areas in order to prevent any of the resulting NURBS curves from intersecting each other or the boundary of the part. If any of these intersections occur, the ANSYS structural analysis module is not able to generate a mesh of the part and compute a solution.

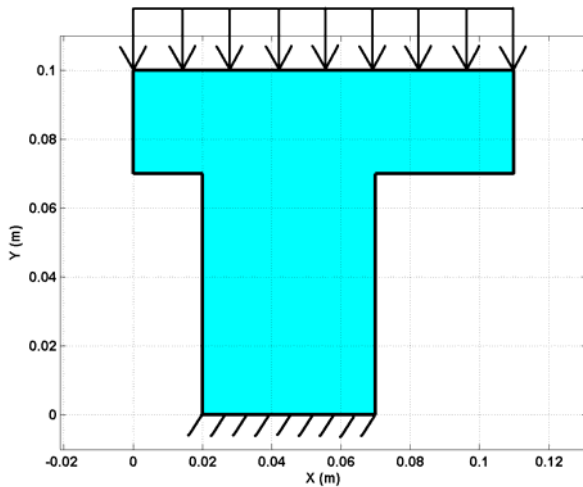


Figure 5: Structural part design with loading and boundary conditions shown.

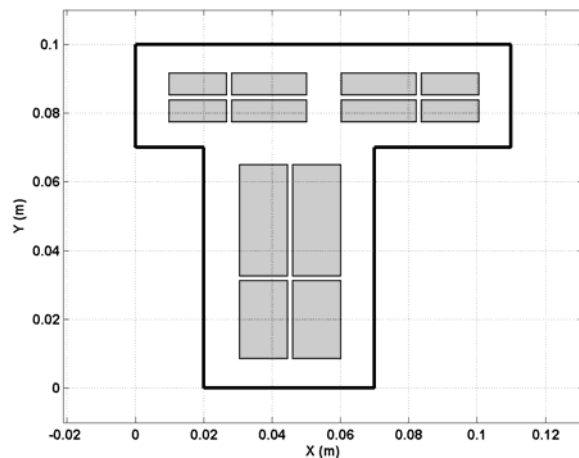


Figure 6: Side constraints of the control points.

Three initial designs are considered during the optimization of this structural part. These three designs are selected to attempt to start the same optimization from significantly different areas of the design space with the goal of finding solutions close to the global optimum. These designs, shown in Fig. 7, include small, medium, and large-sized holes cut in the blank metallic part. Finding a near-global optimal design is done by selecting the “best” design solution of the three produced from starting at the selected initial designs. This is necessary due to the nonlinearity of the objective functions. These “best” design solutions are used to create the Pareto front.

2. Results and Discussion

Selected structural design solutions are shown in Fig. 8. The tradeoff between mass and manufacturing cost can be clearly seen in the results. From Fig. 8 it can be seen that when manufacturing cost is weighted more heavily, the cut-outs in the metallic part are small and the manufacturing cost is low. However, when mass is weighted more heavily, the cut-outs in the part are significantly larger and manufacturing cost is high.

A set of weighting factors of [0.2,0.6,0.65,0.7,0.75,0.8,0.85,0.9,0.95] is investigated. It is observed that the weighted sum design solutions are not in the correct order. It is important to mention that the maximum stress constraint is active for all designs except for the cases of weighting factors of 0.2 and 0.6. The solution from the weighting factor of 0.2 should have lower cost and greater mass than the solution for the weighting factor of 0.6, yet this is not the case. There are two likely causes for this problem. First, it is possible that too few initial designs are

investigated in order to find a near-global optimal design solution. The design solutions found are likely local optima and not global optimal solutions. However, the more likely cause of this problem is that manufacturing cost is not only a function of cutting curve length but also the radius of curvature of the cutting curve. From the manufacturing cost model, a specific radius of curvature limit exists at which cuts with radii greater than the limit are assumed to be at the maximum cutting speed. Below this radius of curvature limit, the cutting speed is slower and not constant and therefore the cost per unit length of material increases. Figure 9 illustrates this radius of curvature limit for manufacturing cost minimization. The example used to illustrate this phenomenon is a comparison of closed circular cuts with varying radii.

An evenly distributed Pareto front is not found in this multiobjective optimization. This phenomenon is likely caused by the fact that the objective functions being minimized are highly nonlinear in terms of the weighting factor, α , and an even distribution of weighting factors is used. The use of the adaptive weighted-sum (AWS) method developed by de Weck and Kim²¹ would alleviate this problem and will be attempted in future work.

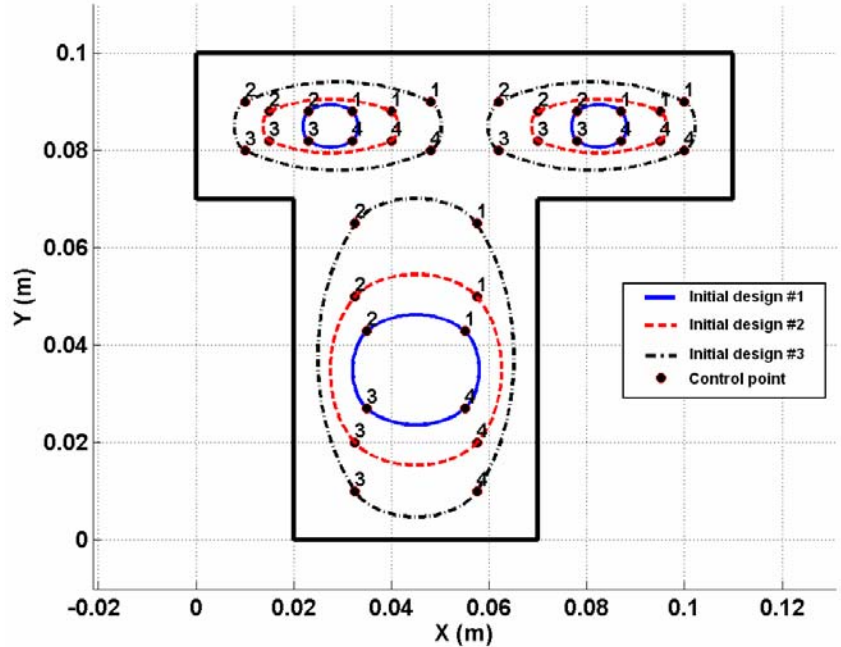
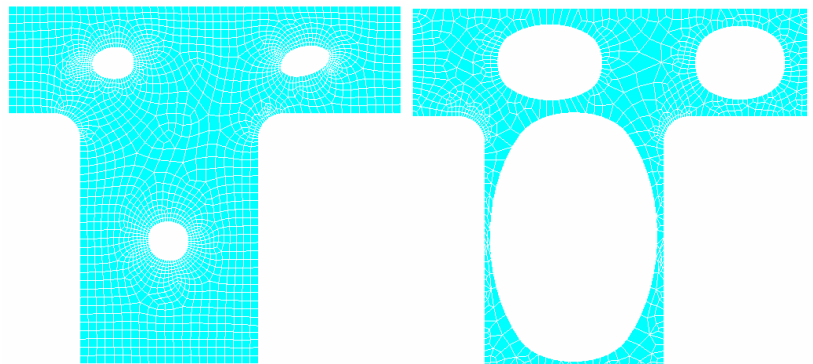


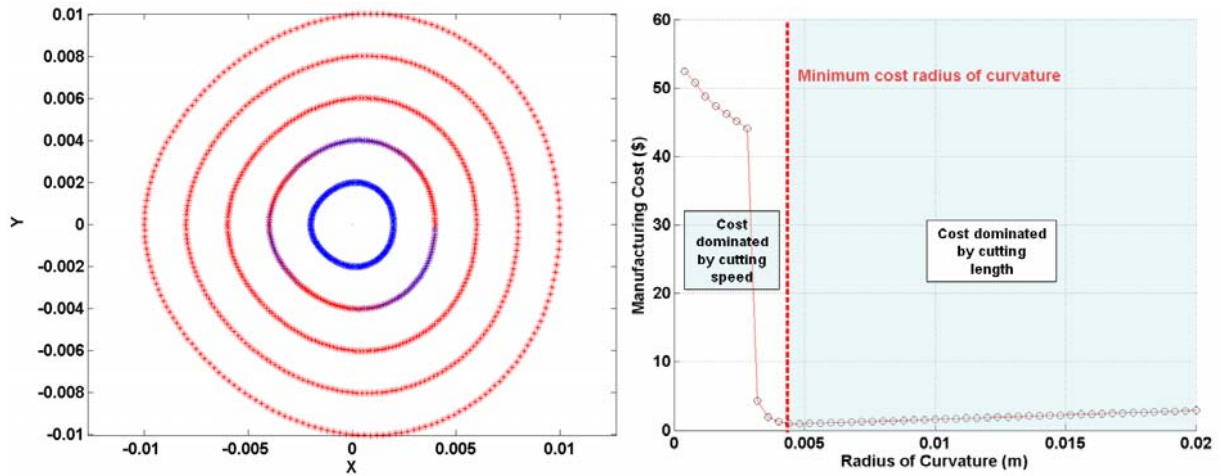
Figure 7: Initial designs considered in the optimization.



a) Weighting factor of 0.2, mass of 0.52 kg, cost of \$3.05

b) Weighting factor of 0.8, mass of 0.21 kg, cost of \$9.10

Figure 8: Two structural design solutions for generic structure example.



a) Cutting speeds for circular cuts of varying radii

b) Manufacturing cost vs. radius of curvature for circular cuts similar to a)

Figure 9: Radius of curvature limit for manufacturing cost minimization.

Figure 9a is an example of the type of curves used to illustrate the minimum manufacturing cost radius of curvature. Bright red-colored points denote the maximum abrasive waterjet cutting speed while darker colors denote slower cutting speeds. Figure 9b shows the minimum manufacturing cost with respect to radius of curvature. A clear minimum manufacturing cost can be seen at the limit of the maximum linear cutting speed. This minimum was obtained from observations of the radius of curvature limit at which Omax software assumed the maximum linear waterjet cutting speed was used for various cutting qualities. Two important trends can be seen in the figure. First, when the radius of curvature is less than the minimum cost radius of curvature and cutting speed dominates the manufacturing cost, manufacturing cost rises dramatically for small reductions in radius of curvature. For radii of curvature larger than this minimum cost radius when cost is dominated by cutting length, manufacturing cost rises slowly with a linear relationship to radius of curvature. The cost model nonlinearity due to the dependence of manufacturing cost on radius of curvature causes difficulty for multiobjective optimization and convergence.

The relative cutting speeds estimated by the AWJ cost model are shown in Fig. 10. It can be seen that most of the cuts made for the selected designs are cut at the maximum linear cutting speed. Only the design with a weighting factor of 0.6 has small portions of the cuts in which the waterjet cutting speed is slowed.

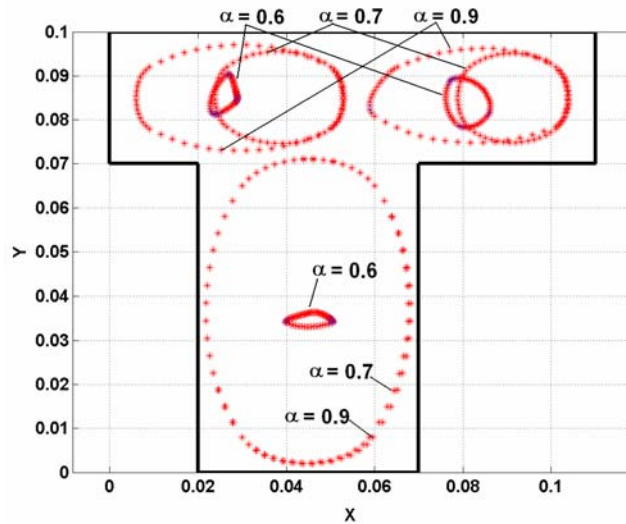


Figure 10: Cutting speeds for selected Pareto front structural designs.

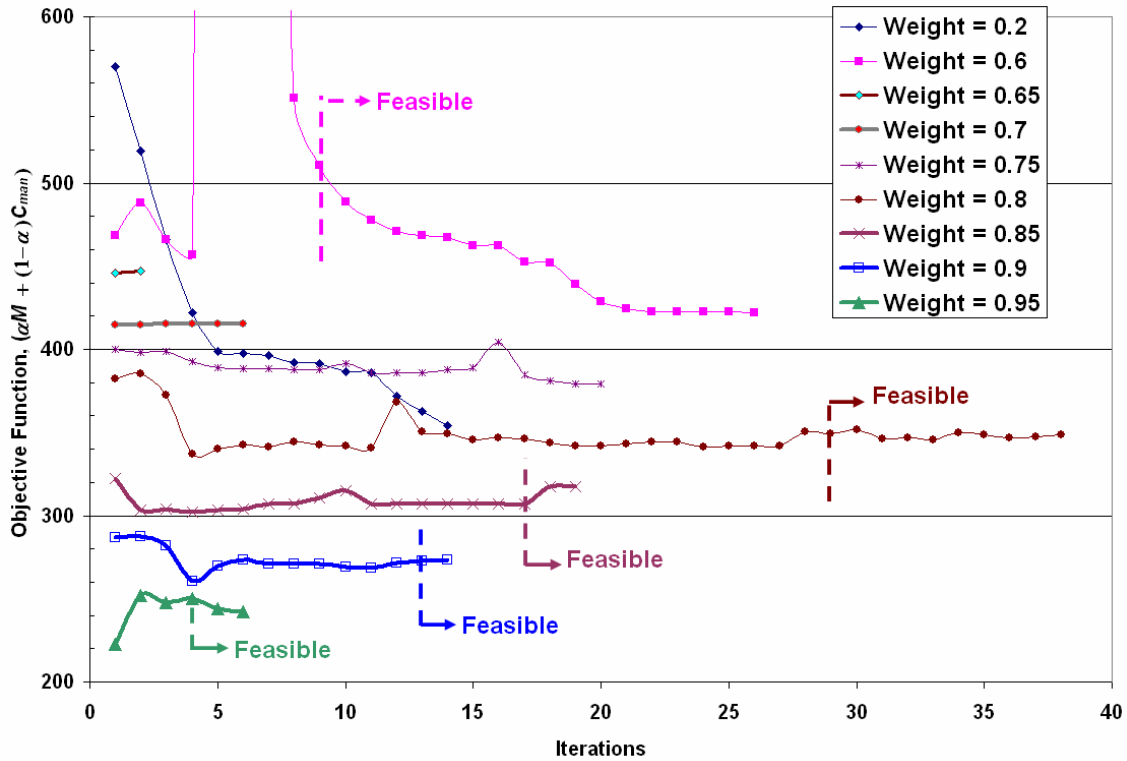


Figure 11: Convergence histories for structural optimization example.

The convergence histories for the optimizations run for each weighting factor are shown in Fig. 11. The designs are all feasible in the figure except where noted. Objective function improvement is more difficult for large weighting factor values. Objective functions with large weighting factors are mass minimization dominant and therefore tend to increase hole sizes. However, the control points defining the NURBS curves for the holes are driven to the side constraints before the stress constraint becomes active. Therefore, the restrictive side constraints are preventing the optimizer from taking full advantage of removal of all structural material and therefore achieving a near-global optimal design.

B. Bicycle Frame Design Optimization

1. Initial Design

Shape optimization considering both structural performance and manufacturing cost is done for a bicycle frame-like part shown in Fig. 12. This structure is roughly 20 by 10 centimeters in size. The material selected for this example is A36 Steel with a Young's modulus of 200 GPa, a Poisson's ratio of 0.26, and a yield strength of 250 MPa. The material thickness is assumed to be 1 cm. A factor of safety of 1.5 was assumed for this example. The loads and restraints applied to the structure are shown in Fig. 12.

The side constraints for each of the control points are shown in Fig. 13. The side constraints are restrictive in order to prevent any of the curves from intersecting with each other or the part boundary. If any of these intersections were to occur, the ANSYS structural analysis module would not be able to properly mesh the part and compute a solution.

Ten curves controlled by three control points each are used to determine the shape of the structure while the structural shape at the vertices of the structure remain unchanged. The relationship of the control points to the curves can be seen in Fig. 14. The cutting path created by the control points is determined using NURBS curves created in ANSYS.

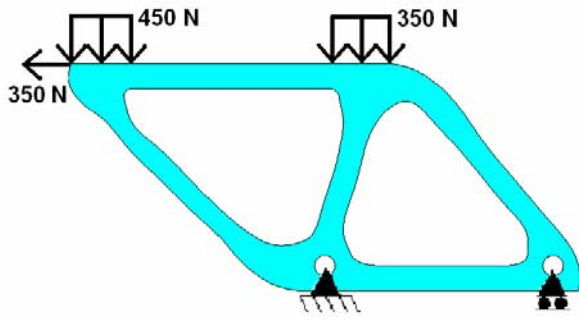


Figure 12: Loads and restraints applied to bicycle frame structure.

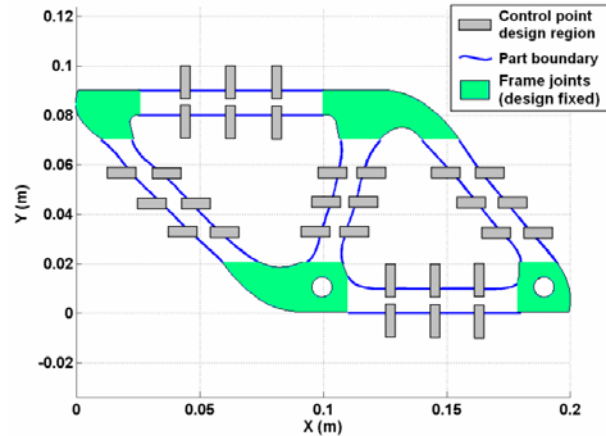


Figure 13: Side constraints of the control points.

Three initial designs are considered during the optimization of this structural part, as is done for the previous optimization example. These designs, shown in Fig. 14, include bicycle frame-like structures with thin, medium, and thick-sized structural members. Finding a near-global optimal design is done by selecting the “best” design solution of the three produced from starting at the selected initial designs. These “best” design solutions are used to create the Pareto front. ANSYS mesh results as well as MATLAB control point locations are shown in the following figure detailing these initial designs.

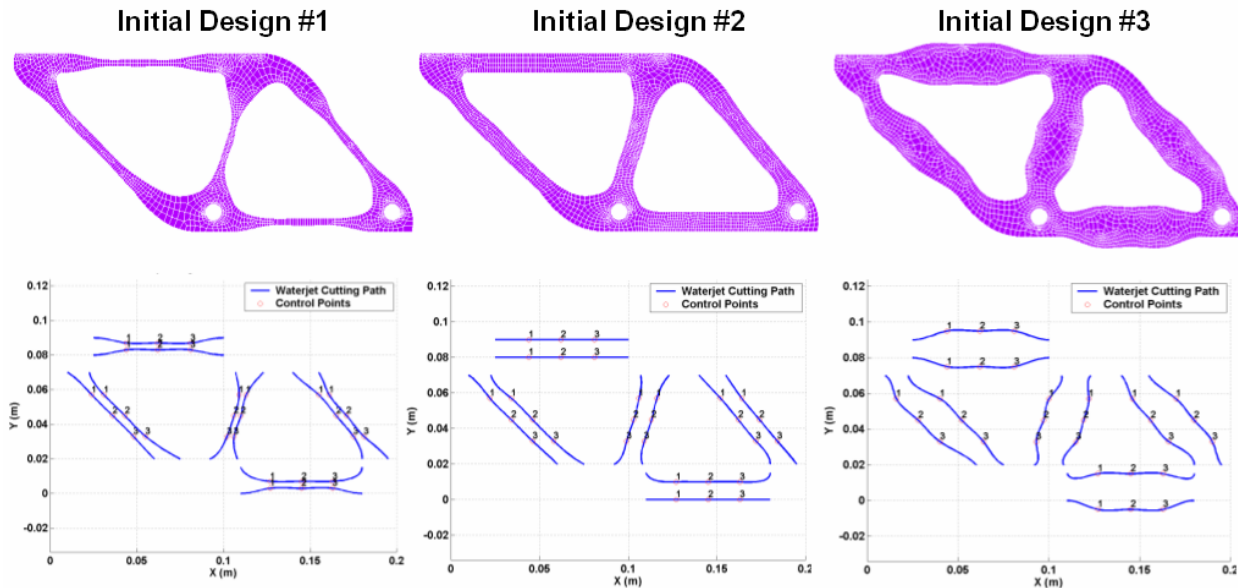


Figure 14: Initial designs considered for the bicycle frame structural optimization example.

2. Results and Discussion

The Pareto front shown in Fig. 15 demonstrates a clear tradeoff between manufacturing cost and mass. It may seem that the improvement in manufacturing cost along the Pareto front is not large. For this example, a manufacturing cost savings of approximately 1.6% is observed when comparing the two anchor points of the Pareto front. However, even a small improvement in manufacturing cost applied to a product being mass produced can have a potentially large cost savings for a manufacturer. In addition, the observed tradeoff between cost and mass should be more significant if the shapes of the bicycle frame joints are included in the design space. Since these pieces of the structure are fixed in size, the cost versus mass tradeoff is restricted for this example.

The maximum stress constraint is not active for any of the resulting structural designs included in the Pareto front. This was a result of the side constraints being restrictive. Design freedom is limited by these side constraints in order to prevent part edge curves from intersecting each other which results in an infeasible design for which structural analysis cannot be performed.

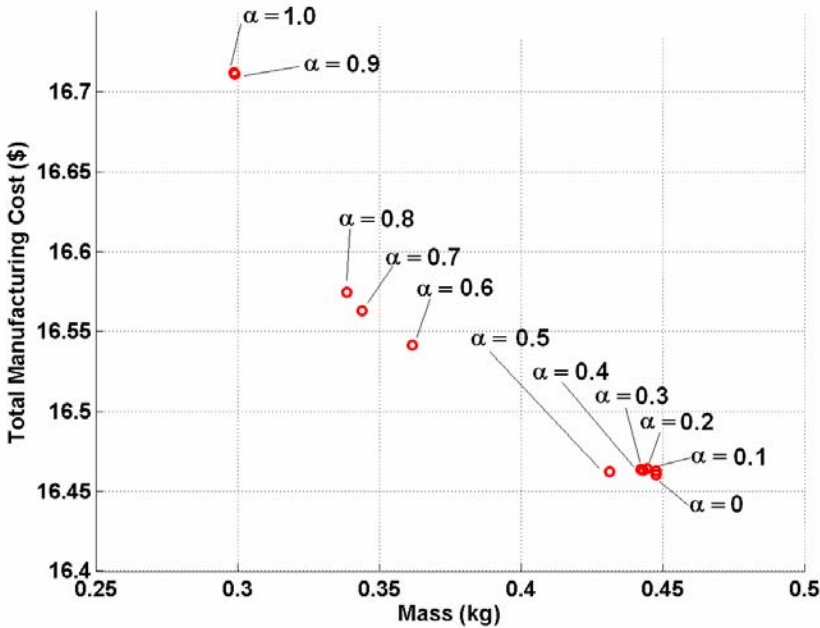


Figure 15: Pareto frontier for bicycle frame structure optimization.

Finally, abrasive waterjet cutting speeds for all designs for this example are calculated to be at the maximum linear cutting speed of the AWJ cutter for the selected example. This results in better results than are obtained for the generic structural part example presented earlier in the paper.

Selected structural designs from the Pareto set are shown in Fig. 16. The tradeoff between objectives can be clearly seen by comparing structural designs for different weighting factors. The design for which the weighting factor is 0.1 results in a structure with nearly straight edges for minimum manufacturing cost. However, the design for a weighting factor of 0.6 results in a design with narrow structural members in order to minimize structural mass. This results in low mass but higher manufacturing cost as a result.

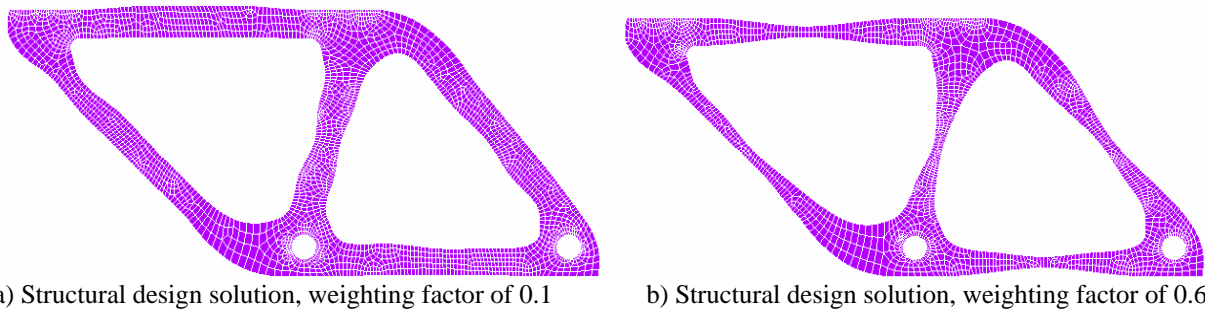


Figure 16: Resulting “optimal” structural designs for various weighting factors.

The abrasive waterjet cutter was used to manufacture one design solution one example. The manufactured part is shown in Fig. 17. The manufacturing cost model was verified with the results obtained from abrasive waterjet machining of the part.

V. Conclusion

Although the area of structural shape optimization is fairly mature, we introduce in this paper the consideration of manufacturing cost in the optimization process. Although a two-dimensional manufacturing process, abrasive waterjet cutting, is selected for this research, other more complicated manufacturing processes can be used as well. Two examples are used to exemplify the application of this procedure for multiobjective structural optimization problems.

The tradeoff between structural performance and manufacturing cost is shown with Pareto fronts for two example metallic parts. Mass is used as the metric for structural performance and maximum stress is the constraint.

VI. Future Work

Future work will primarily deal with including topology optimization in the optimization process. In particular, the optimizer will be given the freedom to determine the number, location, and size of holes in the part while considering the manufacturing cost and structural performance. In addition, future work will include implementing the adaptive weighted sum (AWS) method developed by de Weck and Kim for the generic structural part example. This method should allow for the generation of a well-distributed Pareto front for the example. The bicycle frame example results will be improved by including the bicycle frame joints in the design space by allowing their shapes to be optimized. Additional future work will include performing topology optimization in which the number of curves are considered as a design variable, and the method will be applied to more complicated structures and implementing a new manufacturing cost model. Potential manufacturing process cost models to include are milling and stamping.

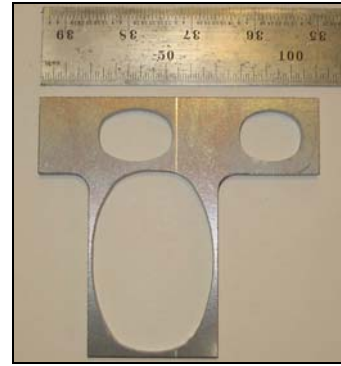


Figure 17: AWJ manufactured generic structural part for weighting factor of 0.7.

References

- ¹ Zolésio, J.P., 1981., "The material derivative (or speed) method for shape optimization," *Optimization of Distributed Parameter Structures*, Sijthoff & Noordhof, Netherlands, pp. 1089-1151.
- ² Haug, E.J., Choi, K.K., and Komkov, V., 1986, *Design sensitivity analysis of structural systems*. Academic Press.
- ³ Bendsøe, M.O. and Kikuchi, N., 1988, "Generating optimal topologies in structural design using a homogenization method," *Comp. Meth. Appl. Mech. Engng.*, Vol. 71, pp. 197-224.
- ⁴ Suzuki, K. and Kikuchi, N., 1991, "A homogenization method for shape and topology optimization," *Comp. Meth. Appl. Mech. Engng.*, Vol. 93, pp. 291-318.
- ⁵ Yang, R.J. and Chuang, C.H., 1994, "Optimal topology design using linear programming," *Comp. Struct.*, Vol. 52 (2), pp. 265-275.
- ⁶ Kim, I.Y. and Kwak, B.M., 2002, "Design Space Optimization Using a Numerical Design Continuation Method," *International Journal for Numerical Methods in Engineering*, Vol. 53, Issue 8, pp. 1979-2002.
- ⁷ Chang, K.-H. and Tang, P.-S., 2001, "Integration of design and manufacturing for structural shape optimization," *Advances in Engineering Software*, 32, pp. 555-567.
- ⁸ Park, C., Lee, W., Han, W., Vautrin, A., 2004, "Simultaneous optimization of composite structures considering mechanical performance and manufacturing cost," *Composite Structures*, Vol. 65, Issue 1, pp. 117-127.
- ⁹ Zadeh, L., 1963, "Optimality and Non-Scalar-Valued Performance Criteria," *IEEE Transactions on Automatic Control*, AC-8, pp. 59-60.
- ¹⁰ Koski, J., 1988, "Multicriteria Truss Optimization," *Multicriteria Optimization in Engineering and in the Sciences*, Ed. by Stadler, New York, Plenum Press, pp. 263-307.
- ¹¹ Zeng, J. and Kim, T., 1993, "Parameter Prediction and Cost Analysis in Abrasive Waterjet Cutting Operations," *Proceedings of the 7th American Water Jet Conference*, Seattle, Washington, August 28-31, pp. 175-189.
- ¹² Singh, P. and Munoz, J., 1993, "Cost Optimization of Abrasive Waterjet Cutting Systems," *Proceedings of the 7th American Water Jet Conference*, Seattle, Washington, pp. 191-204.
- ¹³ Zeng, J., Olsen, J., and Olsen, C., 1999, "The Abrasive Water Jet as a Precision Metal Cutting Tool," *Proceedings of the 10th American Water Jet Conference*, Houston, Texas, August 14-17, pp. 829-843.
- ¹⁴ Zeng, J., 1992, "Mechanisms of Brittle Material Erosion Associated with High-pressure Abrasive Waterjet Processing," *Doctoral Dissertation*, Department of Mechanical Engineering and Applied Mechanics, University of Rhode Island.
- ¹⁵ Zeng, J., Kim, T., and Wallace, R., 1992, "Quantitative Evaluation of Machinability in Abrasive Waterjet Machining," *Precision Machining: Technology and Machine Development and Improvement*, Presented at the Winter Annual Meeting of The American Society of Mechanical Engineers, Anaheim, California, November 8-13, pp. 169-179.
- ¹⁶ Omax Layout, Software Package, Ver. 6.2, Omax Corporation, Kent, WA, 2002.
- ¹⁷ Omax Make: Precision Velocity Controller, Ver. 3.2, Omax Corporation, Kent, WA, 2001.
- ¹⁸ MATLAB, Ver. 6.5, Rel. 13, The Mathworks, Inc., Natick, MA, 2002.
- ¹⁹ ANSYS, Ver. 8.1, Educational Edition, ANSYS, Inc., Canonsburg, PA, 2004.
- ²⁰ Olsen, J., 1996, *Motion Control with Precomputation*, Assignee: Omax Corporation, U.S. Patent 5,508,596.
- ²¹ de Weck, O. and Kim, I.Y., 2004, "Adaptive Weighted Sum Method for Bi-objective Optimization," *Proceedings of the 45th AIAA/ASME/ASCE/AHS/ASC Structures, Structural Dynamics & Materials Conference*, Palm Springs, California, April 19-22.